Article

Tsunami Arrival Detection with High Frequency (HF) Radar

Belinda Lipa [1,*], James Isaacson [2], Bruce Nyden [3] and Donald Barrick [3]

[1] Codar Ocean Sensors, 125 La Sandra Way, Portola Valley, CA 94028, USA

[2] Codar Ocean Sensors, 5 Sunset Trail, Sunset Valley, TX 78745, USA;
E-Mail: jisaac@Austin.rr.com

[3] Codar Ocean Sensors, 1914 Plymouth St., Mountain View, CA 94043, USA;
E-Mails: Bruce@codar.com (B.N.); Don@codar.com (D.B.)

* Author to whom correspondence should be addressed; E-Mail: Belinda@lipa.name;
Tel.: +1-650-851-5517; Fax: +1-408-773-0514.

Abstract: Quantitative real-time observations of a tsunami have been limited to deep-water, pressure-sensor observations of changes in the sea surface elevation and observations of sea level fluctuations at the coast, which are essentially point measurements. Constrained by these data, models have been used for predictions and warning of the arrival of a tsunami, but to date no system exists for local detection of an actual incoming wave with a significant warning capability. Networks of coastal high frequency (HF)-radars are now routinely observing surface currents in many countries. We report here on an empirical method for the detection of the initial arrival of a tsunami, and demonstrate its use with results from data measured by fourteen HF radar sites in Japan and USA following the magnitude 9.0 earthquake off Sendai, Japan, on 11 March 2011. The distance offshore at which the tsunami can be detected, and hence the warning time provided, depends on the bathymetry: the wider the shallow continental shelf, the greater this time. We compare arrival times at the radars with those measured by neighboring tide gauges. Arrival times measured by the radars preceded those at neighboring tide gauges by an average of 19 min (Japan) and 15 min (USA) The initial water-height increase due to the tsunami as measured by the tide gauges was moderate, ranging from 0.3 to 2 m. Thus it appears possible to detect even moderate tsunamis using this method. Larger tsunamis could obviously be detected further from the coast. We find that tsunami arrival within the radar coverage area can be announced 8 min (*i.e.*, twice the radar spectral time resolution) after its first appearance. This can provide advance warning of the tsunami approach to the coastline locations.

1. Introduction

Existing tsunami watch systems are based on computer modeling programs that warn against the possibility of earthquake-generated tsunami impacts, and attempt to predict their strength and arrival times *vs.* location based on the earthquake characteristics [1–3]. These computer models include ocean-scale bathymetry and coastline geometries, with the input parameters updated by ocean bottom pressure as the tsunami wave passes overhead after a potentially dangerous earthquake. A protocol exists for the rapid dissemination of seismic data and tsunami model predictions between foreign governments but no system exists for local detection of an actual incoming wave with a significant warning capability. Tide-gauge sea levels at coastal positions closer to the epicenter do provide useful quantitative information for locations further downstream, if they are able to transmit data. The 2011 Japan tsunami signal was observed by many HF radars around the Pacific Rim with clear results from sites in Japan, US and Chile [4,5]. We here describe and demonstrate an empirical method for the automatic detection of a tsunami based on pattern-recognition in time series of tsunami-generated current velocities, using data measured by fourteen radars [6] on the coasts of Japan and USA. HF radar systems presently operate continuously from many coastal locations around the globe, monitoring ocean surface currents and waves to distances from shore of up to 200 km. Tsunami watch software could run in the background, activating a warning should a tsunami be detected, before the local infrastructure is damaged. World locations of radars [6] are available on http://www.codar.com/ seasonde_world_locations.shtml.

Barrick [7] originally proposed the use of shore-based HF radar systems for tsunami warning. Subsequent analysis refined this concept and a pattern-recognition algorithm was proposed [8] that could be employed using a single radar to detect a tsunami among the background currents. This algorithm was based on the premise that when current velocity components perpendicular to the depth contours are dominated by a tsunami, they would be coherent over area bands parallel to the depth contours. When current velocities from the Japan 2011 tsunami were examined, the assumption of coherence was found to be inaccurate, degrading the utility of the algorithm. Using data measured during the Japan tsunami, we found that plotting the average of radial velocity components over the bands versus time provides a clear signal of tsunami flows: the arrival of the tsunami is indicated by the commencement of distinctive current velocity oscillations [4].

A tsunami is a shallow-water ocean wave that follows linear theory for water depths greater than about 5 m. The shallow-water approximation holds when water depth is much less than the wavelength. In this situation, the wave phase velocity (defined as following a wave crest) is equal to the group velocity (defined to follow the energy transport). Relevant equations for this regime are provided in [4,8]. To provide an example, consider a tsunami with 40-min wave period that is 1 m high in water of depth 500 m. The tsunami wavelength at this depth is 168 km, and its group and phase speed are both 70 m/s or 252 km/h. The orbital velocity, which the radar measures, is 14 cm/s.

As the water depth decreases, the tsunami height increases slowly, as the inverse one-quarter power of depth. The orbital velocity increases more rapidly, as the inverse three-quarters power of depth. Its wavelength decreases as the square root of depth. The phase and group velocities also decrease as the square root of the depth.

A new detection algorithm based on pattern-recognition of the tsunami signal is described in Section 2. Section 3 gives examples of the detection of the Japan tsunami arrival at radar sites around the northern Pacific Rim using the methods described in Section 2. Arrival times at the radars are compared with those measured by neighboring tide gauges. We show that the HF radar systems indeed detected the arrival of the tsunami, representing the first automatic tsunami detection with any radar albeit in hindsight. We note that the tsunami was detected by the radars even though water height amplitude variations seen at nearby tide/wave gauges were moderate, ranging from 0.3 to 2 m in all cases. This detection software is being prepared for deployment, with an alarm threshold level and warning display set to accommodate specific user needs.

A more sophisticated approach under development is to look for pre-determined tsunami spatial patterns in radial current velocities. These spatial patterns are derived from analytical models based on local bathymetry and shoreline configuration.

2. Detection of the Tsunami Signal in HF Radar Data

Methods used to observe the tsunami signal have been described previously [4,8]. In this paper we describe and demonstrate a detection algorithm based on these observations.

To summarize the observation methods: (a) Short-term radar cross spectra (4-min time resolution) are analyzed to give radial velocities; (b) Radial velocities in area bands 2-km wide and approximately parallel to the depth contours are resolved in the direction perpendicular to the depth contour and pointing onshore; (c) These velocity components are averaged over the bands; (d) A time series of the average velocity in each band is formed, which shows the characteristic oscillations produced by the tsunami. Figure 1 gives an example of measured 4-minute radial vectors and the 2-km area bands used in the analysis. We note that such short-term spectra are noisy. For use in processing for current velocities, several spectra are averaged over time. For tsunami detection, unaveraged spectra are used to maximize the resulting time resolution.

Figure 2 shows the averaged velocity component observed at Kinaoshi, Hokkaido, for three 2-km bands ranging from 6 to 12 km from the shore The transmit frequency for this radar is 42 MHz. This frequency band is used for high-resolution, short-range current observations and results in a radar range less than 15 km because of significant attenuation of the surface wave passing across the sea. Figure 2(a) shows the velocities for several hours and displays the characteristic oscillations due to the tsunami. Figure 2(b) isolates the time close to the arrival of the tsunami. Two effects distinguish tsunami velocities from the background: (i) after arrival within the area monitored, velocities in neighboring bands are strongly correlated and (ii) the oscillation magnitudes increase significantly above background values.

Figure 1. Radial current velocities from the Usujiri, Hokkaido radar and the area bands used in the analysis which are 2-km wide and approximately parallel to the depth contours.
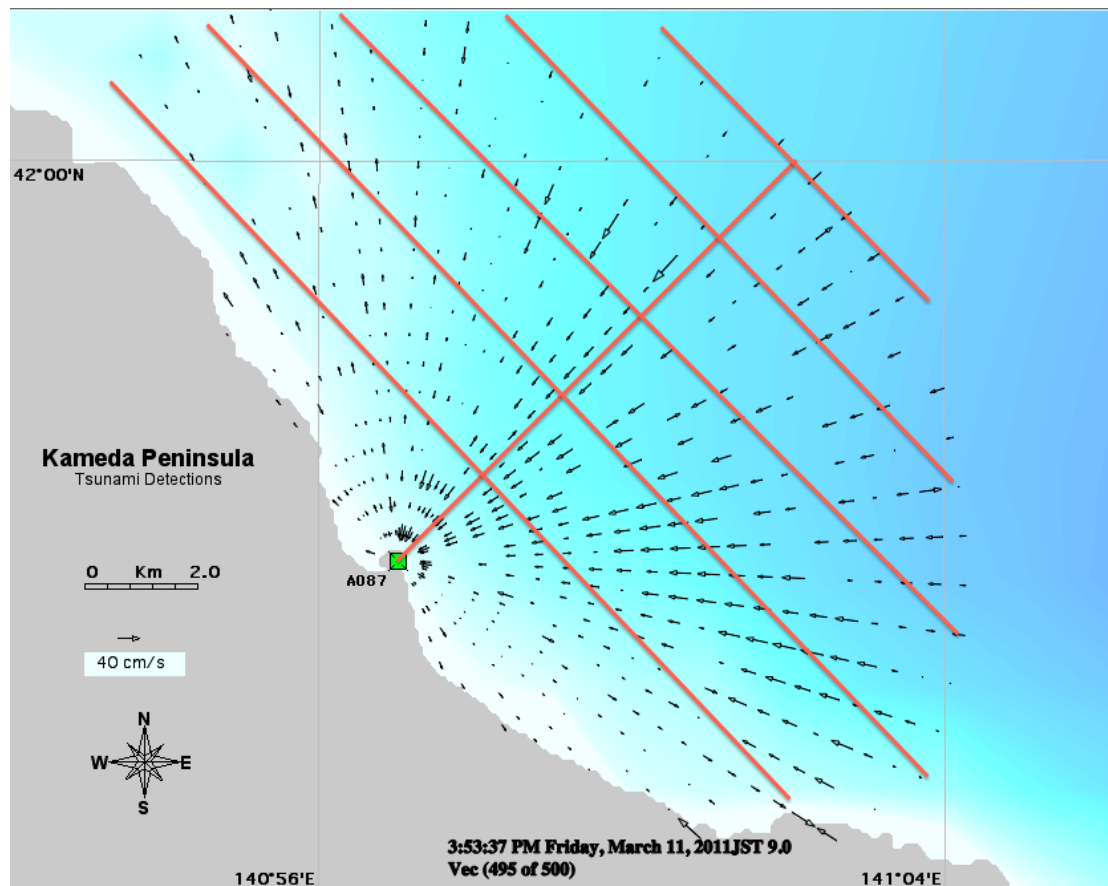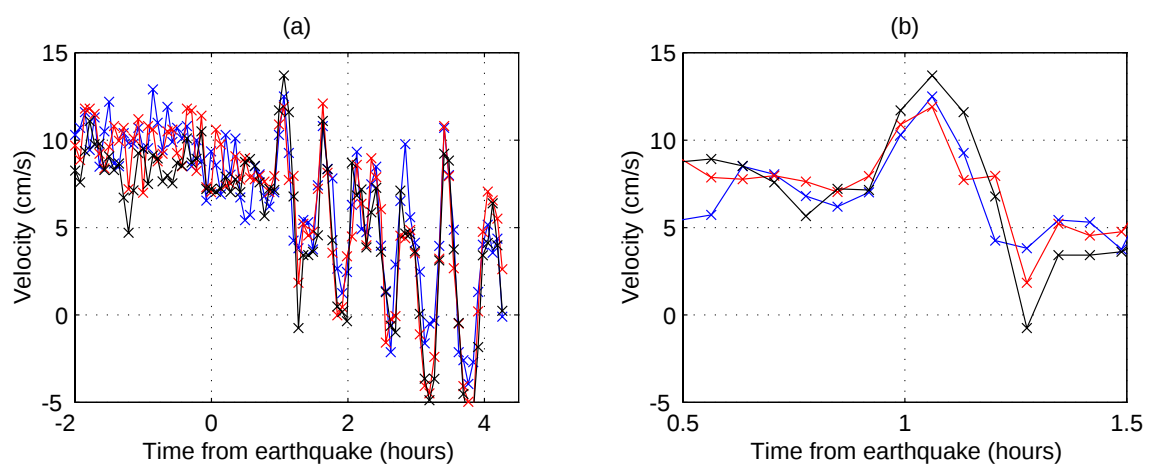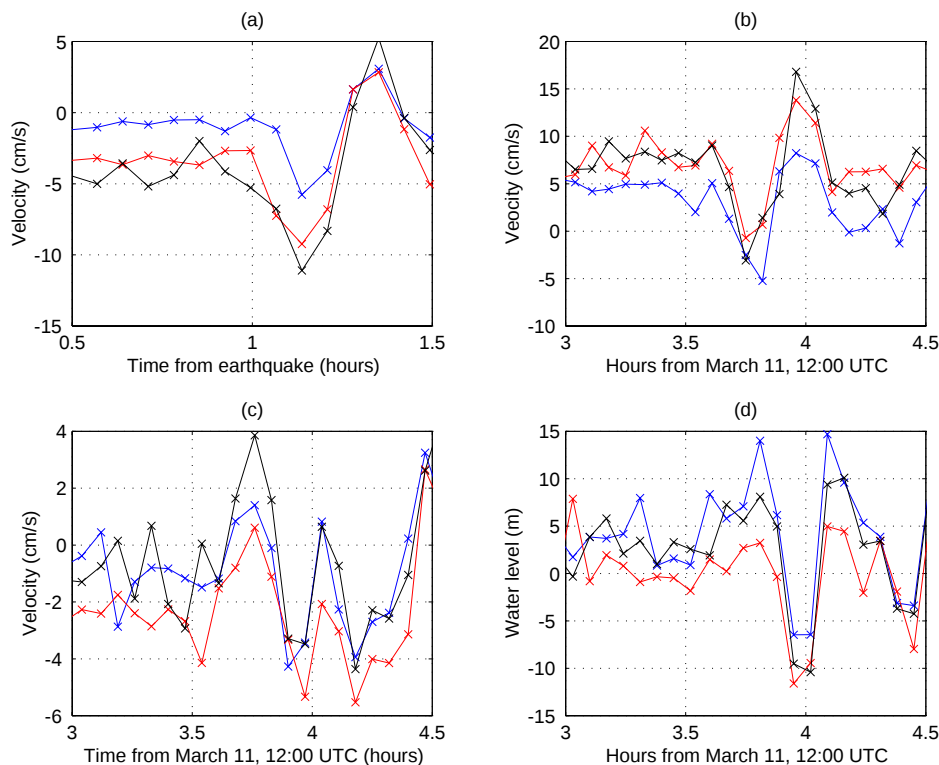
Figure 2. Time series of current velocity components from the Kinaoshi radar. Radial current velocities were resolved perpendicular to the area band boundaries, and averaged. Area bands used were 2 km wide and approximately parallel to the depth contours. Blue: 6–8 km; Red: 8–10 km; Black: 10–12 km. (**a**) From 2 h before the quake until 5 h after. (**b**) Around the tsunami arrival.

The effects (i) and (ii) are seen in all the radar data we have examined from Japan and the US West Coast; further examples are shown in Figure 3 below. Locations of the radars are shown in Figures 4 and 7.

Figure 3. Time series of averaged velocity components showing the typical appearance around the tsunami arrival for three adjacent 2-km area bands. (**a**) A087 (Hokkaido, Japan, JST); (**b**) YHS2 (OR, USA, UTC); (**c**) BML1 (CA, USA, UTC); (**d**) PREY (CA, USA, UTC).

We developed the following pattern detection procedure based on these signal characteristics. At a given time, a factor (which we call the q-factor) is defined which signals the tsunami arrival when it exceeds a preset threshold. Velocities at three adjacent times and three area bands are examined for correlations as follows:

(i) For band b at time t, calculate the average $a_b(t)$ and standard deviation $s_b(t)$ of the velocity $v_b(t)$ over the preceding hour.

(ii) For each band, calculate a measure of the velocity deviation from the background

$$d_b(t) = \frac{(v_b(t)\text{-}a_b(t))}{s_b(t)}$$

The velocity deviation function D(t) at time t is defined to be the product over the bands:

$$D(t) = \prod_b d_b(t) \tag{1}$$

(iii) For each band, calculate the change in velocity over two adjacent time intervals from $t - 2\delta$ to t, where δ is the time resolution of the input data:

$$\Delta v_b(t) = v_b(t) \text{-} v_b(t\text{-}2\delta)$$

The velocity increment function $\Delta V(t)$ is defined to be the sum over the bands:

$$\Delta V(t) = \sum_b \Delta v_b(t) \tag{2}$$

(iv) Calculate a correlation function C(t) describing the correlation between velocities in three adjacent bands over times t, $t - \delta$, $t - 2\delta$, where δ is the time resolution of the input data. The correlation

function C(t) is set to unity, unless the velocity increases or decreases with time for all three area bands from $t - 2\delta$ to $t - \delta$, and $t - \delta$, to t, when it is defined to be 100.

(v) The tsunami detection factor at time t is defined to be the product of the correlation function, the velocity increment function and the velocity deviation function:

$$q(t) = C(t) \cdot \Delta V(t) \cdot D(t) \tag{3}$$

3. Application to Radar Data

In this section, we give examples of the detection of the Japan tsunami arrival at radar sites around the northern Pacific Rim using the methods described in Section 2. Arrival times at the radars are compared with those measured by neighboring tide gauges.

3.1. Japan
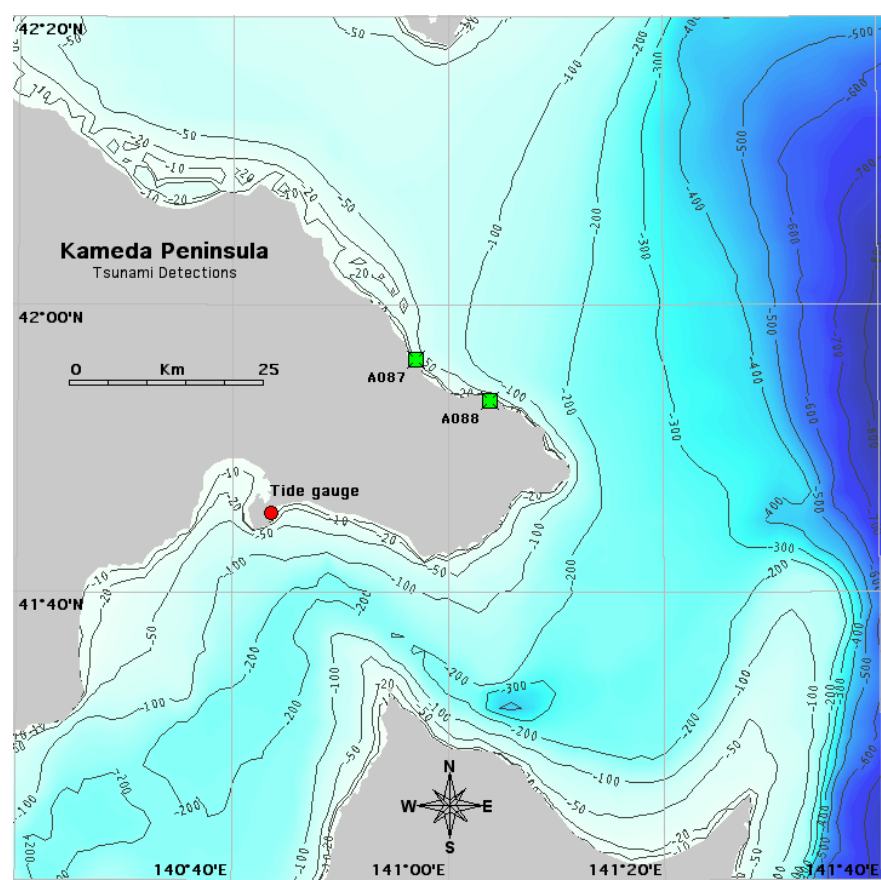
Figure 4 shows the locations of the instruments in Japan that produced the data used in this study: two radars on the Kameda Peninsula, two radars on the Kii channel and neighboring tide/wave gauges. Also shown is the offshore bathymetry. The water depth is less than 200 m over the radar coverage area; we find that the tsunami signal is visible in the current velocities to the radar range limits.

Figure 4. (**a**)The general location of the Japan earthquake and the radars in Hokkaido and on the Kii Strait. Both locations were sufficiently far from the epicenter to experience only moderate disturbances. (**b**) The bathymetry offshore from the Radars A088, A087 on the Kameda Peninsula, Hokkaido and the tide gauge at Hakodate. (**c**) The bathymetry offshore from the Radars TOKU, ANAN on Shikoku and the KO seabed wave gauge.
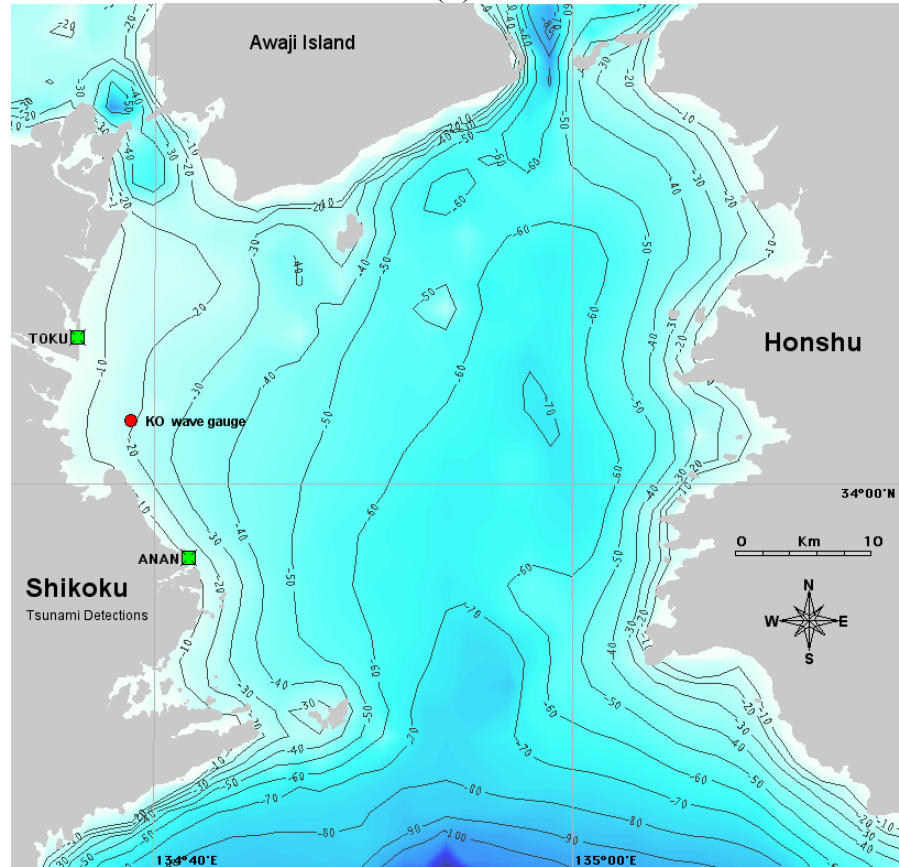
(**a**)

Figure 4. *Cont.*

(**b**)
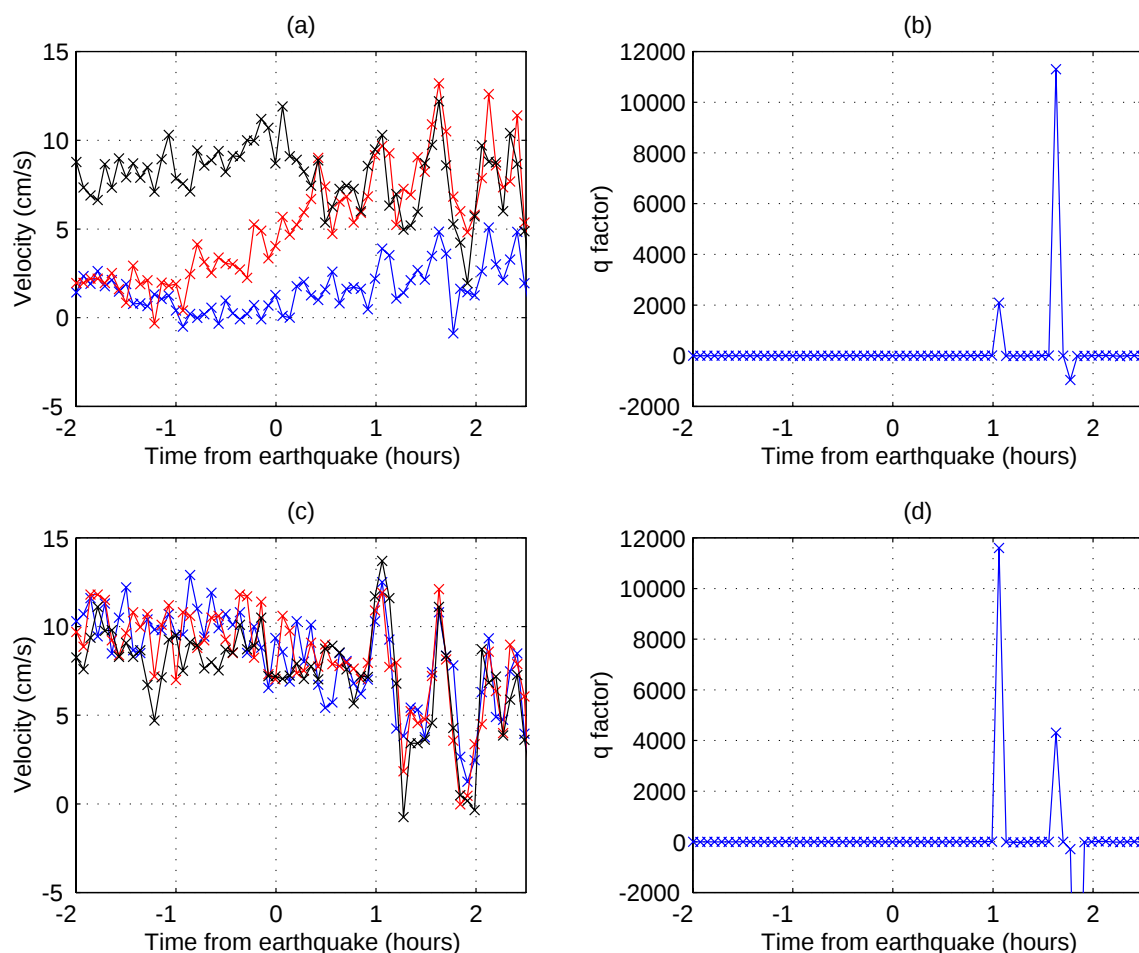
(**c**)

Examples follow of velocity components measured in Japan and the derived q-factors which indicate the tsunami arrival.

3.1.1. Kinaoshi, Hokkaido (A088)

Figure 5 shows the velocities in six 2-km area bands measured by A088 and the corresponding q-factors. The tsunami arrives about an hour after the earthquake, as indicated by the correlation in the velocities in the different bands. This results in a sharp increase in the q-factor, indicating the tsunami arrival. The tsunami signal is particularly clear in the bands further from the radar; closer to shore the flow is diverted parallel to shore, reducing the perpendicular component shown in these plots.
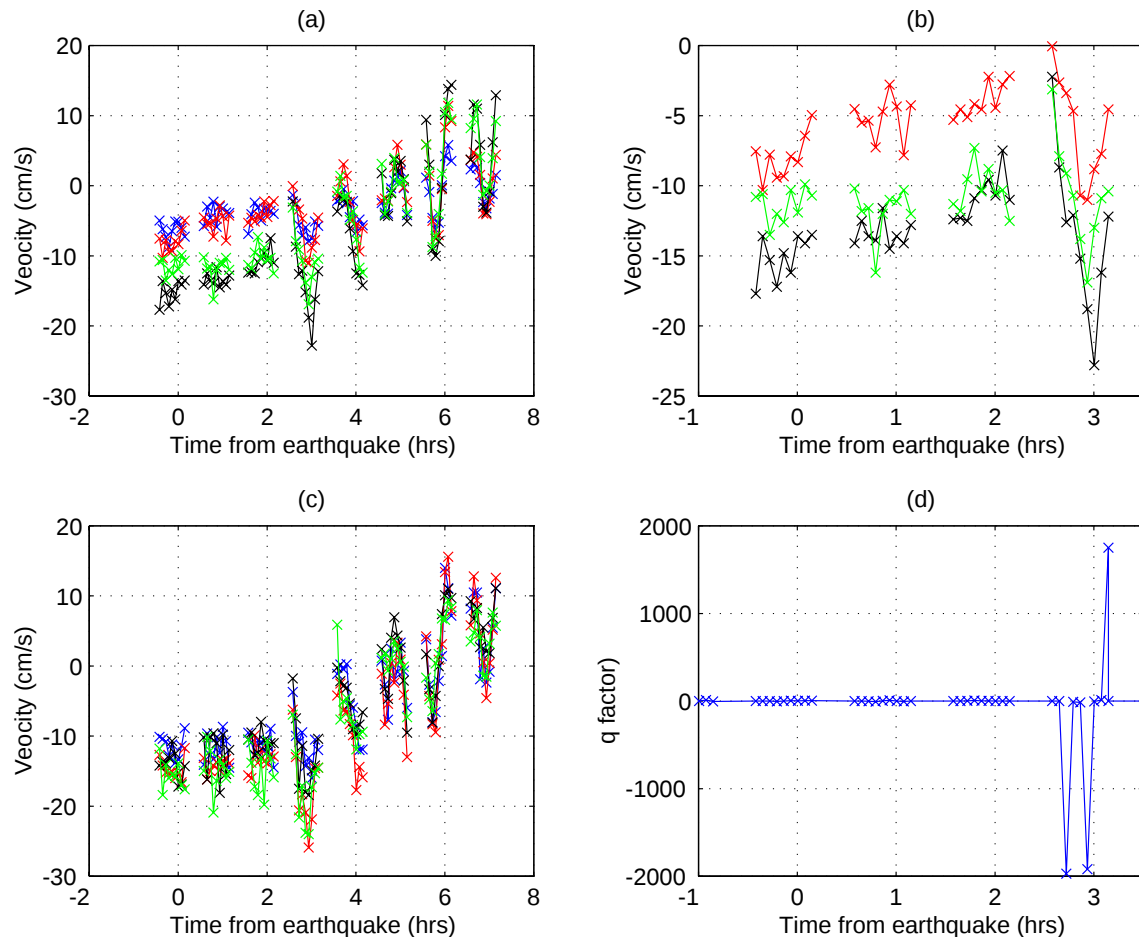
Figure 5. Time series of velocity components from radar A088. (**a**) Blue: 0–2 km; Red: 2–4 km; Black: 4–6 km over 5 h (**b**) q-factor for 0–6 km offshore (**c**) Blue: 6–8 km; Red: 8–10 km; Black: 10–12 km (**d**) q-factor for 6–12 km offshore.

3.1.2. Tokushima, Japan (TOKU)

Figure 6 shows the velocity components for the first eight 2-km bands. The radar transmit frequency is 25 MHz. Also shown is the q-factor for three of these bands.

Figure 6. Time series of velocity components from TOKU. (**a**,**b**): Blue: 0–2 km; Red: 2–4 km; Black: 4–6 km; Green 6–8 km (a) over 10 h (b) around the tsunami arrival time (**c**) Blue: 8–10 km; Red: 10–12 km; Black: 12–14 km; Green 14–16 km. (**d**) q-factor for 2–8 km offshore.

This radar operates for only 40 min in the hour, resulting in the 20-min gaps visible in the plots. (The radar is turned off every hour for 20 min to avoid interference with an NJRC radar on the opposite shore, which operates at that time.) The water depth is less than 70 m over the whole radar coverage area and the tsunami signal is visible to the outer radar range. The arrival of the tsunami is indicated by correlation between velocities in different bands starting about 2.5 h after the earthquake. As the normal procedure for calculating the velocity deviation factor was invalidated by the time gaps in the input data, instead of (3) the q-factors for TOKU and ANAN were defined to be:
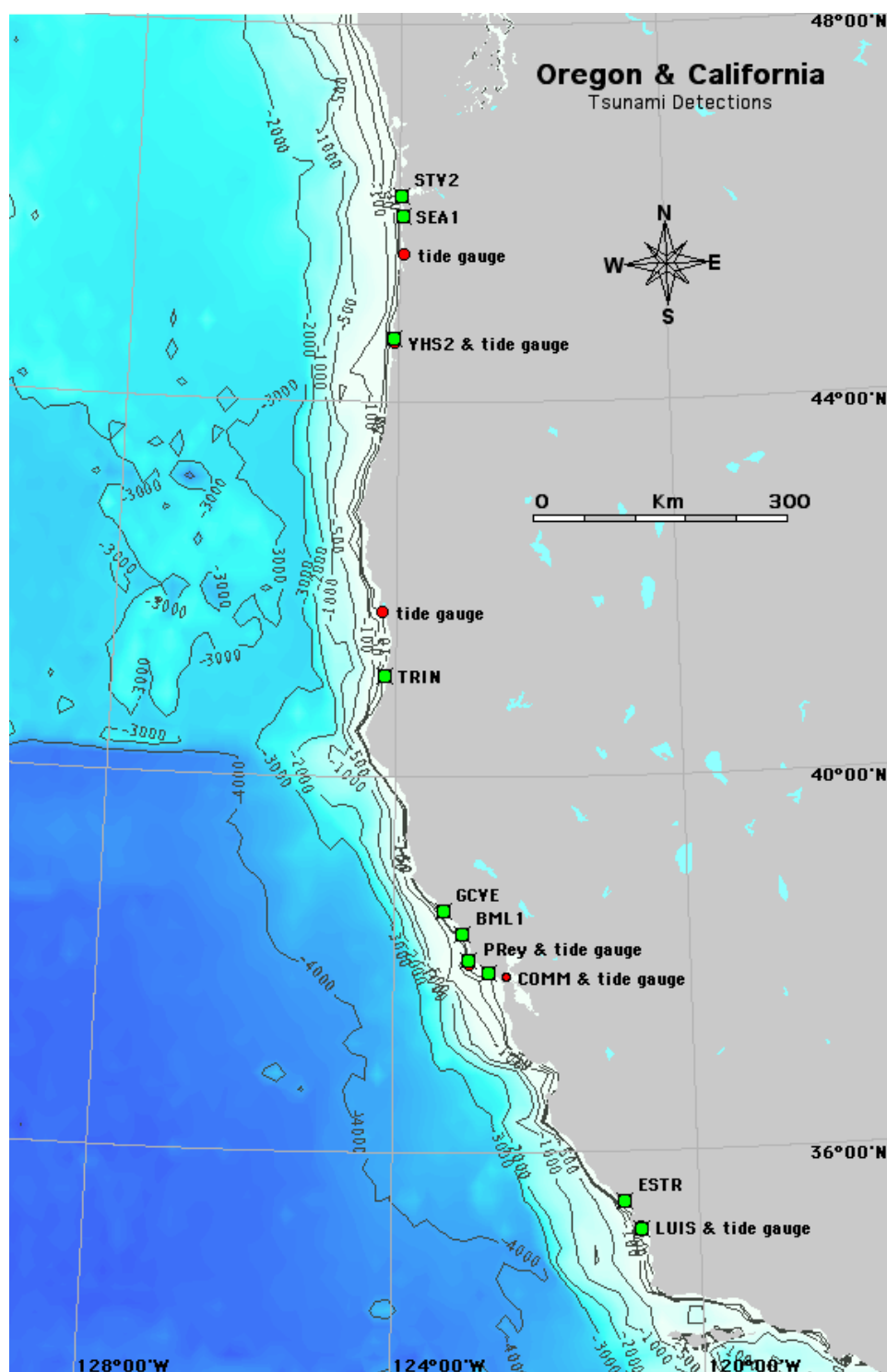
$$q(t) = C(t) \cdot \Delta V(t) \tag{4}$$

The q-factor shows a sudden change in magnitude about 8 min after the start of the velocity correlations. At this point, the velocity is decreasing, indicating that the tsunami is moving offshore, resulting in the negative q-factor as shown in Figure 5(d). KO seabed wave gauge readings shown in Figure 2 of reference [5] indicate that the initial approach of the tsunami produces an increase in water height, which would correspond to an increasing current velocity. Therefore it appears that the initial tsunami approach actually occurred during the preceding 20-min gap when the radar was not operating.

3.2. US West Coast

We have analyzed data from ten radars located along the coast from Oregon to Southern California with typical ranges of 100 km, or more. Their locations are shown in Figure 7 along with those of neighboring tide gauges and the offshore bathymetry. The continental shelf is narrow here, particularly for much of California. The tsunami signal is often evident only in the closer ranges to the radar.

Figure 7. The location of the radars and tide gauges on the US West Coast, and the offshore bathymetry.
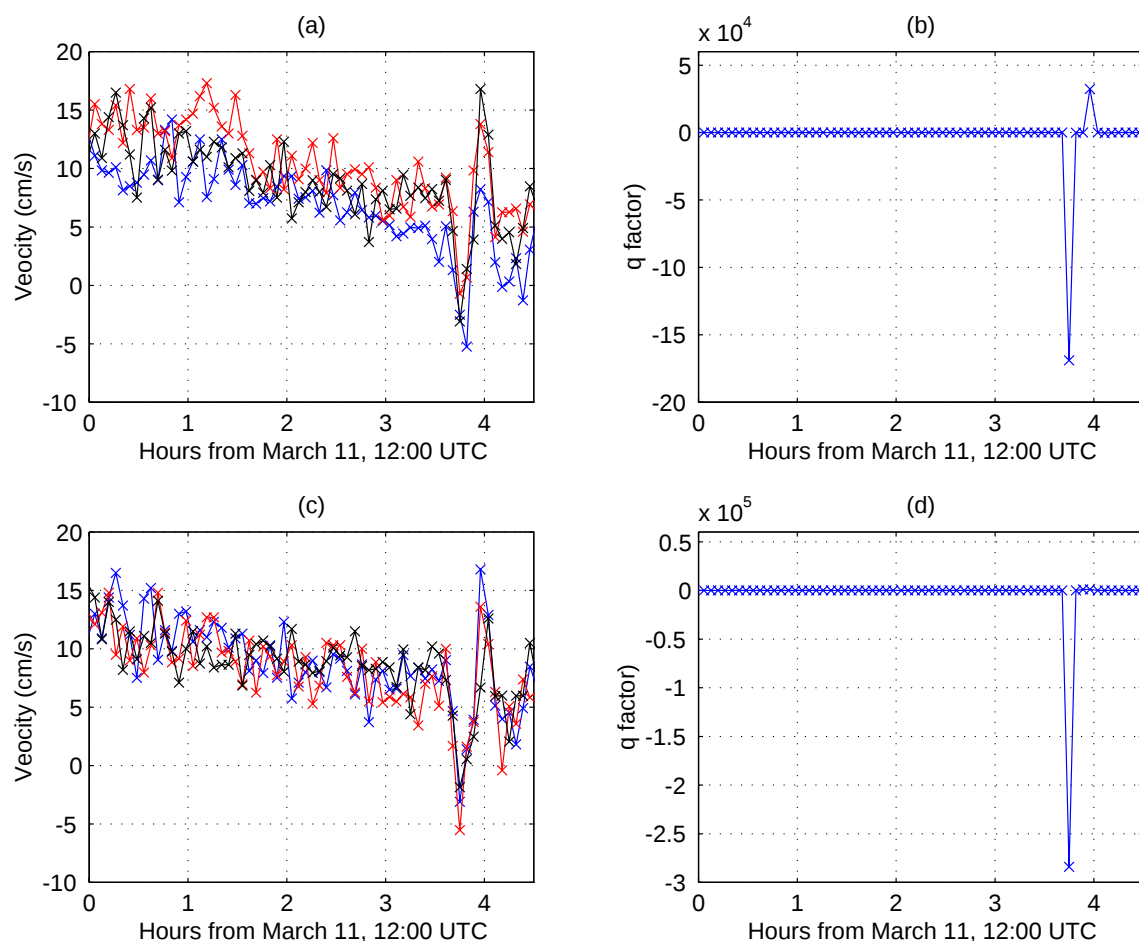
We now give examples of measured velocity components and the derived q-factors that indicate the tsunami arrival.

3.2.1 Yaquina Head South, Oregon (YHS2)

Figure 8 shows the averaged velocities in 2-km area bands. The radar transmit frequency was 12 MHz. The correlation is evident between the velocities in different bands starting at about 3:45 pm UTC. This results in the sharp decrease observed in the q-factor, indicating the presence of the tsunami. Tide gauge measurements along the US West Coast show increasing water height at the onset of the tsunami; the initial water level increase due to the tsunami at the neighboring South Beach tide gauge was only 0.3m. It appears that this was too small to allow our algorithm to pick up the tsunami's initial approach. In fact the increasing velocity is visible in Figure 8(a,c) just before the sharp decrease.
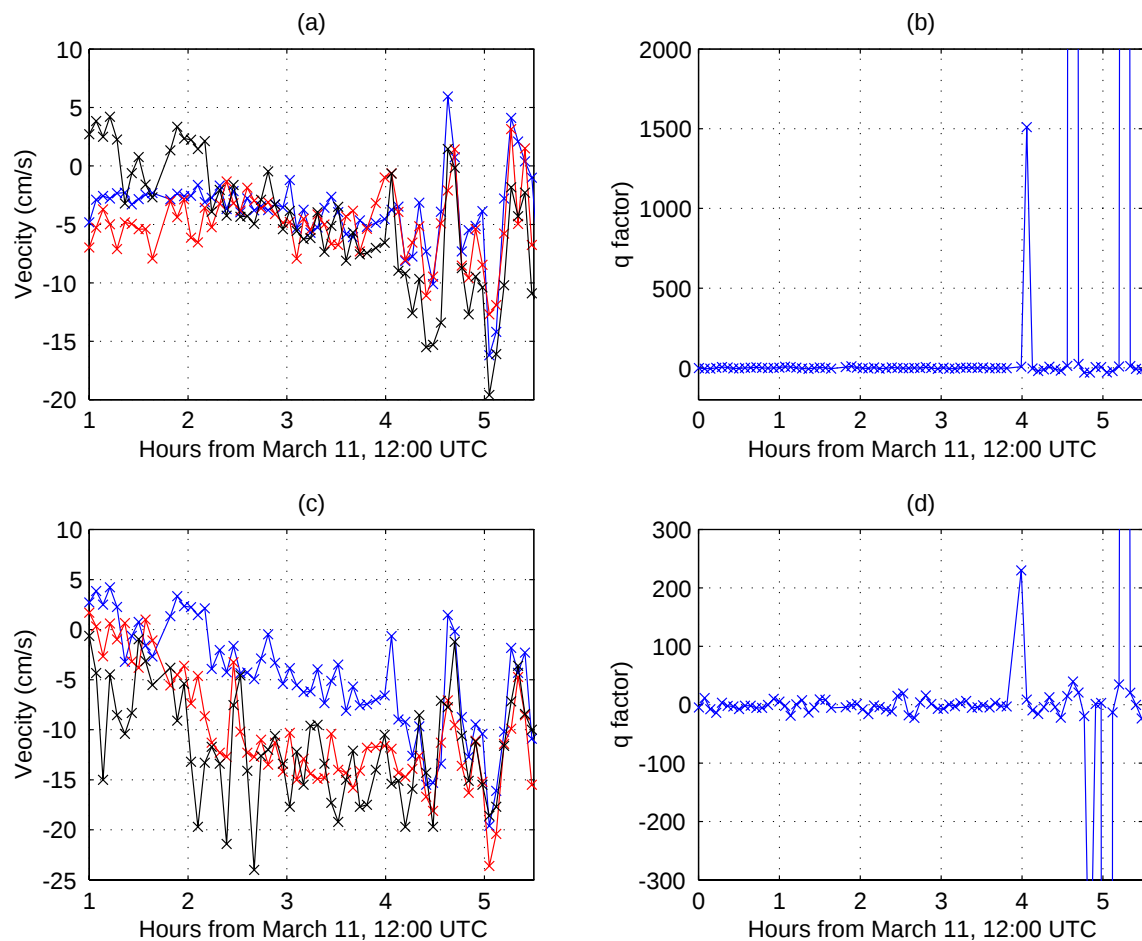
Figure 8. Time series of velocity components from radar YHS2 (**a**) Blue: 2–4 km; Red: 4–6 km; Black: 6–8 km (**b**) q-factor for 2–8 km (**c**) Blue: 8–10 km; Red: 10–12 km; Black: 12–14 km (**d**) q-factor for 8–14 km offshore.

3.2.2 Point Estero, California (ESTR)

Figure 9 shows the averaged velocities in 2-km area bands. The radar transmit frequency was 13 MHz. The observed background current velocities are quite variable for this site: it is the correlations between velocities in different bands that allow the tsunami to be detected.

Figure 9. Time series of velocity components from radar ESTR (**a**) Blue: 2–4 km; Red: 4–6 km; Black: 6–8 km (**b**) q-factor for 2–8 km offshore (**c**) Blue: 8–10 km; Red: 10–12 km; Black: 12–14 km. (**d**) q-factor for 8–14 km offshore.

3.3. Comparison between Arrival Times Measured by Radar and Tide Gauge

For the comparison, the procedure described in Section 2 was applied to the fourteen radar sites for all permutations of three area bands displaying the tsunami signal, and the resulting q-factors summed. The radar arrival time was defined to be when the magnitude of the sum exceeded 500. The first tsunami peak at the tide/wave gauge was taken to define the arrival time. The comparison is shown in Table 1. The Japan tsunami took approximately 10 h to reach the US West Coast; computed travel times indicate that it moved down the coast from North to South, see http://www.ngdc.noaa.gov/hazard/honshu_11mar2011.shtml. Radar stations are listed in the order of the expected arrival of the tsunami.

Table 1. Comparison of tsunami arrival times from radars and neighboring tide/wave gauges.

Japan 11 March 2011 JST				
Radar (XMTR Freq)	*Arrival Time (JST)*	*Ground Instrument*	*Arrival Time (JST)*	*Water-Level Change*
A088 (42Mhz)	15: 49	Hakodate tide gauge	16:32	2.0 m
A087 (42Mhz)	15: 54	Hakodate tide gauge	16:32	2.0 m
TOKU* (25Mhz)	17:29	KO* wave gauge	17:24	0.5 m
ANAN* (25Mhz)	17:25	KO* wave gauge	17:24	0.5 m

US West Coast 11 March 2011 UTC				
Radar (XMTR Freq)	**Arrival Time (UTC)**	**Tide Gauge**	**Arrival Time (UTC)**	**Water-Level Change**
STV2 (12 MHz)	15:32	Garibaldi	15:48	1.2 m
SEA1 (12 MHz)	15:47	Garibaldi	15:48	1.2 m
YHS2 (12 MHz)	15:45	South Beach	15:54	0.3 m
TRIN (5 MHz)	15:34	Crescent City	15:48	0.5 m
GCVE (14 MHz)	15:44	Pt. Reyes	16:00	0.5 m
BML1 (12 MHz)	15:46	Pt. Reyes	16:00	0.5 m
PREY (13 MHz)	15:49	Pt. Reyes	16:00	0.5 m
COMM (13 MHz)	15:56	Fort Point	16:30	0.4 m
ESTR (13 MHz)	16:04	Port San Luis	16:24	2.0 m
LUIS (13 MHz)	16:05	Port San Luis	16:24	2.0 m

Arrival times measured by the radars preceded those at neighboring tide gauges by an average of 19 min (Japan)* and 15 min (USA), due to the "quadrature relation" [4] between velocity and height (*i.e.*, velocity precedes height by a quarter cycle due to the coastal boundary condition), and the tsunami propagation delay between the two observations. We expect to be able to quantify the propagation delay when spatial tsunami velocity patterns derived from analytical models become available.

*As discussed in Section 3.1.2, the tsunami initially arrived at TOKU and ANAN slightly before the time shown here, during one of the periods when the radar was not operating. The arrival time we report here probably defines the subsequent tsunami retreat from the coast. The tsunami arrival time at the wave gauge KO was estimated from Figure 2 of reference [5].

The table shows that listed arrival times obtained from the radar q-factors reported are normally in the correct order, e.g., the tsunami arrives at Station A087 approximately five minutes after it reaches A088; it arrives in Southern California after it gets to Northern California and Oregon. We note that TOKU, ANAN are the only radars for which the q-factor arrival time was later than that seen at the relevant tide gage, which is probably due to the intermittent operation of those radars.

4. Conclusions

We have described an empirical method to detect tsunami arrival, which has been applied to radar data measured by fourteen radars operating during the 2011 Japan tsunami. Using this method, we find that tsunami arrival within the radar coverage area can be announced approximately 8 min (*i.e.*, twice the radar spectral time resolution) after its first appearance. This can provide advance warning of the tsunami approach to the coastline locations when the water depth is less than 200 m. We note that the initial water-height increase due to the tsunami as measured by the tide gauges was moderate, ranging from 0.3 to 2 m. Thus it appears possible to detect even moderate tsunamis using this method. Larger tsunamis could obviously be detected further from the coast, with increased advance warning.

We expect to improve the analysis by incorporating additional known tsunami characteristics to produce earlier detection and cut down on the risk of false alarms. An immediate improvement is expected when velocities within site-specific bathymetric contours are used for tsunami analysis rather than fixed rectangular bands used at present. Also improved statistics would be possible when multiple sites cover a common area. A promising deterministic approach is to look for pre-determined tsunami

spatial patterns in radial current velocities. These spatial patterns are derived from analytical models based on local bathymetry and shoreline configuration. This more sophisticated technique is under development.

The analysis software returns a q-value every four minutes. In practice, an alarm is triggered when a preset value is exceeded, which would remain active for a period selected by the user and be reinforced by subsequent high q-values produced by continuing tsunami oscillations.

While there is no doubt that tsunami arrivals have been detected in the data from Japan and California, they were detected only a short time before impact on the shore. This is due to the short range of the Japan radars and the narrow continental shelf off the western US coast. Nevertheless the results show promise for improved offshore detection. Using similar methods in ongoing studies, we can now provide accurate estimates of the warning times for other regions, e.g., the US east coast, South East Asia and the west coast of India, where shallow-water bathymetry extends well offshore. High frequency (HF) radar installations at such locations will provide vital capability for the detection and measurement of the local intensity of deadly approaching tsunamis.

Acknowledgments

References

1. Titov, V.V. Tsunami forecasting. In *The Sea*, Chapter 12; Harvard University Press: Cambridge, MA, USA and London, UK, 2009; Volume 15, pp. 371–400.
2. Wei, Y.; Bernard, E.N.; Tang, L.; Weiss, R.; Titov, V.V.; Moore, C.; Spillane, M.; Hopkins, M.; Kânoğlu, U. Real-time experimental forecast of the Peruvian tsunami of August 2007 for US coastlines. *Geophys. Res. Lett.* **2008**, *35*, L04609.
3. Titov, V.V.; González, F.I.; Bernard, E.N.; Eble, M.C.; Mofjeld, H.O.; Newman, J.C.; Venturato, A.J. Real-time tsunami forecasting: Challenges and solutions. *Natural Hazards* **2005**, *35*, 41–58.
4. Lipa, B.; Barrick, D.; Saitoh, S.-I.; Ishikawa, Y.; Awaji, T.; Largier, J.; Garfield, N. Japan tsunami current flows observed by HF radars on two continents. *Remote Sens.* **2011**, *3*, 1663–1679.
5. Hirofumi, H.; Fujii, S., Furukawa, K.; Kataoka, T.; Miyata, M.; Kobayashi, T.; Mizutani, M.; Kokai, T.; Kanatsu, N. Propagating tsunami wave and subsequent resonant response signals detected by HF radar in the Kii Channel, Japan. *Estuar. Coastal Shelf Sci.* **2011**, *95*, 268–273.
6. Codar Ocean Sensors. *SeaSonde*; Available online: http://www.codar.com/SeaSonde.shtml (accessed on 15 May 2012).
7. Barrick, D.E. A coastal radar system for tsunami warning. *Remote Sens. Environ.* **1979**, *8*, 353–358.
8. Lipa, B.; Barrick, D.; Bourg, J.; Nyden, B. HF radar detection of tsunamis. *J. Oceanogr.* **2006**, *2*, 705-716.